Hindawi
Advances in Civil Engineering
Volume 2022, Article ID 4714420, 11 pages
https://doi.org/10.1155/2022/4714420

Research Article

Experimental Study on the Influence of Type of Stirrup of Prestressed Concrete Beams with Corroded Rebars

Fang-Yuan Li, Liu-Yang Li, Wen-Hao Li, and Peifeng Wu

Department of Bridge Engineering, Tongji University, Shanghai 200092, China

Correspondence should be addressed to Fang-Yuan Li; fyli@tongji.edu.cn

Received 25 January 2022; Revised 30 March 2022; Accepted 8 April 2022; Published 30 April 2022

Academic Editor: Shangtong Yang

Corrosion of longitudinal reinforcement and stirrup in reinforced and prestressed concrete beams is very common for structures and infrastructures, which is one of the main reasons for the decrease in stiffness and durability of structure. In order to evaluate the influence of corrosion of different types of stirrups on the bearing capacity of the prestressed concrete beam, the method of using electricity to accelerate corrosion was adopted. Load experiment on 4 corroded prestressed concrete beams with different corrosion rates and different stirrup types was carried out. In this paper, reduced scale model beams were designed based on the 5×50 m simple-continuous box girder of the Donghai Bridge. The results show that for prestressed concrete beams with different corrosion rates and stirrup types, the load-deflection curve can be divided into an elastic stage and a plastic stage. The corrosion of longitudinal bars and stirrups will reduce the flexural capacity, but the overall decline is not obvious. When the corrosion rate is 10%, the bearing capacity of the ordinary stirrup specimen decreases by 6.1%; epoxy-coated stirrup specimen decreases by 4.9%; stainless stirrup specimen has nearly no change. The influence of different types of stirrups on cracking load, deflection, and bond-slip behavior is discussed.

1. Introduction

Reinforced concrete structure has been widely used in modern buildings because of its low cost, high compressive strength, and good durability. Generally, reinforced concrete structures do have better durability than steel structures. However, with more thorough study since the middle and late 20th century, it was found that carbonation, chloride ion erosion, steel corrosion, and other factors will significantly reduce the service life of concrete structures [1]. Mehta also put forward: "The causes of concrete damage in descending order of importance are steel corrosion, freezing damage, physical and chemical effects of erosive environment" [2]. Nowadays, steel corrosion is surely the most problematic issue of concrete bridges [3], which has been confirmed by a large number of engineering examples. In recent years, the research on durability tends to be complex, comprehensively considering multiple factors including the influence of the environment and load coupling on the deterioration of concrete structure [4].

For the research of steel corrosion, the earliest researchers started from the corrosion of longitudinal steel bar rather than stirrup. The conservative value of ultimate bending moment or ultimate shear force can be predicted by using RC conventional model and considering the reduction of reinforcement and concrete section caused by corrosion of reinforcement [5, 6]. Mangat believed that the decrease in flexural strength of corroded beams was mainly caused by the breakdown of the bond at the steel/concrete interface [7]. In addition to affecting the bearing capacity of the structure, steel corrosion can change the failure mode [8] and significantly increase the fundamental frequency and damping ratio of the structure [9]. It is worth noting that sometimes the corrosion of stirrups is more serious than that of longitudinal reinforcement. Shi found that sometimes when the corrosion rate of longitudinal reinforcement is only 5%–10%, the stirrup corrosion is very serious [10]. Therefore, stirrup corrosion is very common in concrete structures and has a great impact on the degradation of concrete components.

This paper focuses on the degradation of the bearing capacity of members after stirrup corrosion, and many scholars have done a lot of research work about this problem. Rodriguez studied the shear bearing capacity of corroded reinforced concrete beams through theoretical analysis based on an experiment [5], which laid a foundation for the research of failure mode [6], service life prediction, and evaluation of corroded concrete beams. Stirrup corrosion has an obvious impact on the mechanical performance of the beam and changes the failure mode [11], reducing the shear and deformation behavior performance [12]. There were some new models established to calculate the shear bearing capacity. An analytical model for cross-sectional analysis and shear strength prediction [13] and a method of the whole process analysis showing the shear behavior of reinforced concrete beams with corroded stirrups [14] were developed. Design equations were also proposed to predict the shear strength of corroded RC columns after strengthening [15]. It is more meaningful to combine the calculation model and method with the current design code [16, 17] so as to improve the shear design of concrete beams. In summary, the main factors affecting the shear bearing capacity are shear span ratio, corrosion degree, and stirrup type [18]. The effect of the different stirrups on the shear strength depends on the corrosion degree of stirrup and shear span-to-depth ratio of the beam.

However, the above research on the influence of corroded stirrups of reinforced concrete structure was limited to the shear capacity of beams and bearing capacity of concrete columns under eccentric load. There was almost no research on the influence of corroded stirrups on the bending capacity. Generally speaking, stirrups are mainly used to provide shear strength of inclined section in concrete structures, but they hardly contribute to the flexural capacity of members. But in the case of steel corrosion, the above conclusion is not necessarily true because stirrup corrosion will reduce the restraint capacity of concrete in the core area, resulting in the degradation of the bearing capacity and ductility of the structure [19]. Mander [20, 21] developed a stress-strain model for concrete subjected to uniaxial compressive loading and confined by transverse reinforcement. However, most models did not take into account the stirrup corrosion. Based on the well-established Mander model, modification factors were introduced to predict the constitutive relationship of concrete confined with corroded stirrups [22]. Based on the regressive analysis of the experimental data of 15 reinforced concrete prisms, Liu et al. [23] proposed a stress-strain constitutive model of corroded stirrup confined concrete under axial compression. Moreover, some studies [24] show that the restraint effect of corroded stirrups on concrete is weakened, which leads to the decline in the seismic performance of the structure. Above all, the corrosion of stirrups will change the constitutive relationship, failure mode, and crack distribution of members. So, it is necessary to study the influence of corroded stirrups on the flexural capacity of beams.

For the prestressed reinforced concrete structure, the proportion of ordinary reinforcement is small, so the influence of reinforcement corrosion on the bearing capacity of members may be limited. But the bond failure of reinforcement-concrete caused by reinforcement corrosion and the corroded expansion cracking of concrete in the tension zone will have an impact on the early stiffness. At present, the research on reinforcement corrosion is mostly focused on reinforced concrete structure, while less work has been done to investigate prestressed structure with reinforcement corrosion. Compared with the reinforced concrete structure, the concrete strength grade of prestressed structure is higher (C40 and above); the protective layer is thicker, and the cross-sea bridge is mostly 40 mm; the steel strength is higher, and due to the effect of prestress, the steel bar is in a certain stress state. Through the fatigue test of 9 model beams, Yu found that the static load bearing capacity of prestressed concrete beams is similar to that of ordinary beams without corrosion, as long as the reinforcement does not rust off [25].

In order to measure the strain of corroded steel bars in the loading test, a common method is to slot the steel bars along the longitudinal direction and stick the strain gauges inside. Moreover, during the whole process of energized accelerated corrosion, specimens are in a humid environment, so the survival rate of strain gauge cannot be guaranteed. Due to the differences between prestressed concrete structures and reinforced concrete structures, it is necessary to apply the latest test methods to study the corroded prestressed concrete members based on the actual engineering.

2. Model Beam Design

In this paper, the realization of reinforcement's corrosion was carried out through a method of accelerating corrosion by electricity, which was a commonly used method in the current experiments to study the performance of corroded reinforced concrete members. In fact, whether the specimen was immersed in a solution or placed in the atmosphere, electrifying the steel bars in concrete to accelerate corrosion was an electrolytic process. The positive pole of the external DC power supply was connected to the steel bar to be corroded in concrete, making it act as the anode of the electrolytic cell, and the negative pole of the power supply was connected with stainless steel or carbon rod, making it act as the cathode of the electrolytic cell. A loop was formed to connect the anode and the cathode to react by immersing the sodium chloride solution, thereby accelerating the corrosion of steel bars. Because the anode and cathode of steel bars in the concrete were separated, the corrosion speed was faster and the oxygen supply was insufficient, anode products were all Fe^{2+}, and the corrosion products were distributed more uniformly.

2.1. Specimen Design. The specimens used the 5×50 m simple-continuous box girder of the Donghai Bridge as the prototype (Figure 1), in order to be more realistic and make the results more credible. For the sake of facilitating the production and loading of specimens, the prototype beam was simplified to an equivalent T-shaped beam (Figure 2), and the scale ratio was 1/8.

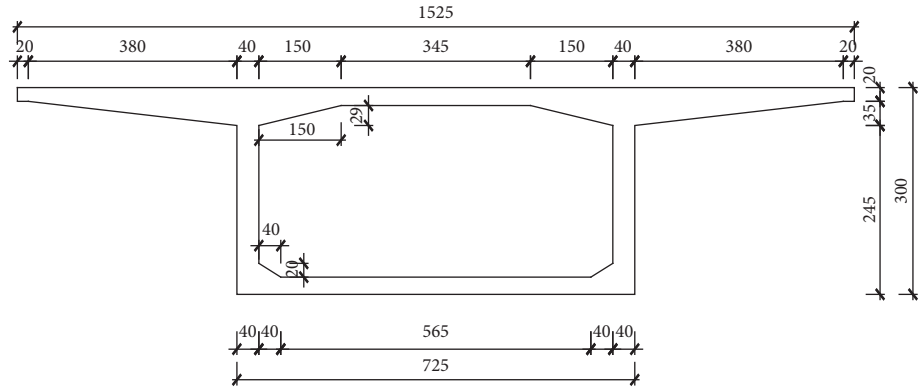

Figure 1: Midspan cross section of 5×50 m simple-continuous box girder of Donghai Bridge (mm).

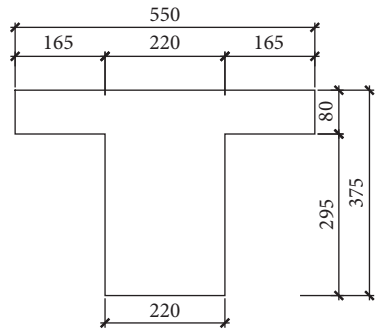

Figure 2: Midspan cross section of model beam (mm).

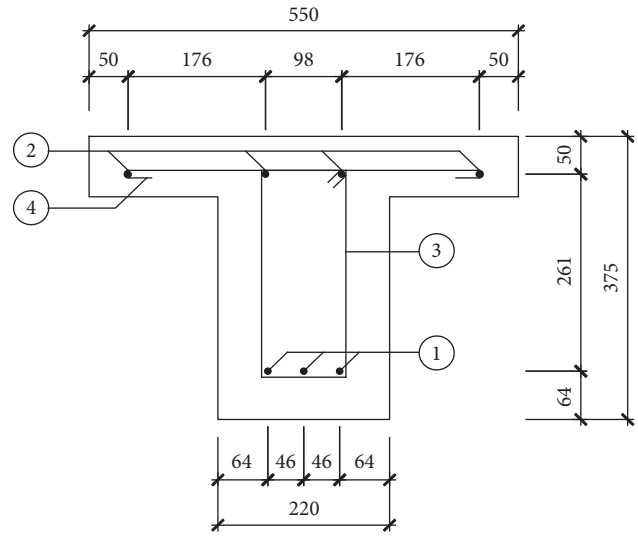

Figure 3: Reinforcement of model beam (mm).

If the principle of scale was strictly followed, the model beam will be as long as 6.25 m, which was expensive to manufacture. Considering that the main purpose of the test was to study the bending performance of the model beam, the beam only needs to meet the loading requirements to avoid shear failure caused by too small shear span ratio and had enough pure bending sections to observe conveniently. Taking 4 prestressed reinforced concrete simply supported beams with a length of 3300 mm and a height of 375 mm as the research objects (Figures 3 and 4), the lower part of the test beam was equipped with three longitudinal steel bars with a diameter of 16 mm without hooks. The reinforcement used in the stirrup was the same as the longitudinal reinforcement, and the spacing was 200 mm, which was 0.64 times the effective height of the beam. The thickness of the protective layer was 40 mm according to the requirements of the reinforced concrete beam structure. The concrete strength grade was C50, and the mix proportion was shown in Table 1. In order to enhance the conductivity of concrete, the specimens were immersed in an electrolytic cell containing 5% sodium chloride solution for 7 days before the energization test, which can greatly reduce the resistance of concrete. The prestressed tendons were steel strands with a nominal diameter of 15.2 mm and a tensile strength of 1860 MPa, and the tensile control stress was 1395 MPa.

The test control variable was the type of stirrups. The corrosion of different types of stirrups had different effects on the degradation of the bond between corroded steel bars and concrete. This test used three types: ordinary stirrups, epoxy-coated stirrups, and stainless stirrups (Table 2). On the basis of some previous work, the corrosion rate of longitudinal bars was determined to be 10%, and the energization was terminated when this target was reached. The name of the specimen was defined in 0P10 as an example, which was composed of longitudinal reinforcement corrosion rate (0), stirrup type, and beam stress state (10 MPa). P, B, and H represented ordinary stirrups, stainless stirrups, and epoxy-coated stirrups, respectively. In addition, the reinforcements of the specimen 0P10 were not rusted by energizing and served as a blank comparison group.

2.2. Specimen Fabrication and Electric Corrosion. The corrugated pipes were tied to the short steel bars welded to the stirrups, in order to avoid the corrosion of the steel strands caused by the later electrification. Epoxy was applied to the outside of the metal corrugated pipes for insulation. In order to measure the bond-slip between the corroded longitudinal bars and the concrete and the stress history of the corroded reinforcement during the loading process, before pouring the specimens, shallow grooves of steel bars were made to bury the fiber grating sensor (Figures 5 and 6).

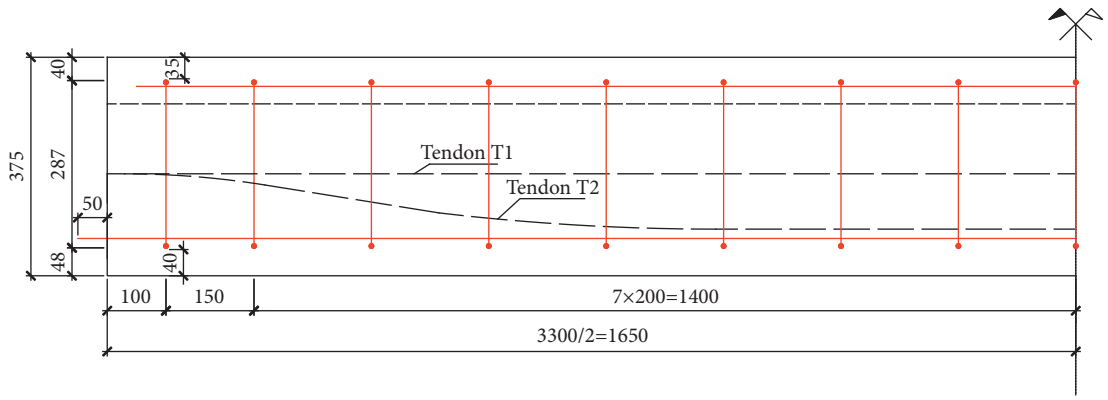

Figure 4: Arrangement of prestressed tendons of model beam (mm).

Table 1: Mix proportion of concrete.

Materials	Water	Cement	Sand	Top	Fly ash	Additive	Mineral powder
Type	Tap water	52.5PII	Medium sand	5–25 mm	Grade II	SPS-8P	S95
Usage (kg/m^3)	83	254	819	1053	72	4.65	97

Table 2: Overview of specimens.

Number	Corrosion rate (%)	Type of stirrup	Stress (MPa)
0P10	0	Ordinary	10
10P10	10	Ordinary	10
10B10	10	Stainless	10
10H10	10	Epoxy-coated	10

Figure 5: A groove of longitudinal reinforcement.

Figure 6: Arrangement of FBG.

The positive pole of the DC power supply was connected to the rusty longitudinal bars, and the cathode was connected to the carbon rod immersed in the solution to form a loop. In order to accurately control the degree of corrosion,

Figure 7: Electric corrosion.

Figure 8: Rust products ooze out.

each beam was equipped with an independent constant DC power supply with a current density of 800 μA/cm^2 as shown in Figures 7 and 8. For the full immersion energization test, when the sodium chloride concentration reached 5%, the electrolysis efficiency was about 80%. In this test, the concrete strength was higher, the protective layer was thicker, and the lower edge concrete was in a higher compressive stress state.

Figure 9: Loading test.

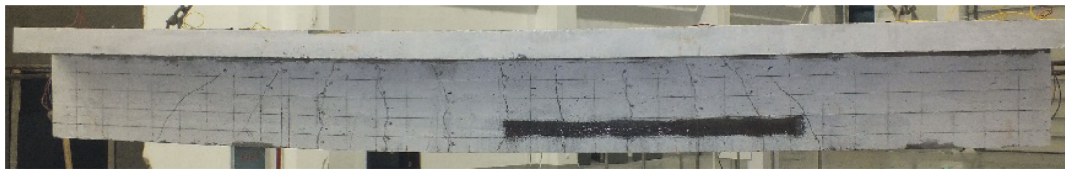

Figure 10: Distribution of 0P10 cracks.

2.3. Loading Test. As shown in Figure 9, the test used three-point loading. In order to avoid the unevenness of the upper edge of the concrete causing the load asymmetry, a layer of fine sand should be laid under the loading pad. In order to eliminate the gap between the loading equipment and the test beam to ensure the normal operation of the test instrument, preloading was carried out before the formal loading, and the level was 40 kN. After the preloading was confirmed to be correct, the formal loading began. Force control was applied in the early stage of loading.

Before reaching 80% of the calculated cracking load (120 kN), the load was carried out according to one step of 40 kN; then, it is loaded according to the step of 10 kN, and the crack development is observed by holding the load for several minutes. When the number of cracks does not increase, the load was applied at 20 kN per step. When the load is close to 80% of the calculated ultimate load (400 kN), the displacement control loading is adopted according to one step of 3 mm. When the load is close to the ultimate load (450 kN), the load is carried out 2 mm per step until the specimen is destroyed. During the test, load, strain gauge, and midspan displacement were automatically collected by dynamic acquisition equipment, and optical fiber data were collected by FBG optical fiber modulation and demodulation instrument. In order to facilitate later data processing, the sampling frequency was set to 1 Hz.

3. Results and Analysis

3.1. Failure Modes and Characteristics. The 11 cracks of the comparison beam 0P10 are relatively regular, with a spacing of about 20 cm (Figure 10), which is closer to the calculation result using code for design of concrete structures [26] (equation (1)). Because of the thick protective layer of the specimen (40 mm), the relatively upper tensile steel, and the wide flange of T-beam (550 mm), the height of the compression zone is very small under the ultimate state of the bearing capacity. Then, the specimen bends extremely obviously, whose limit width of the crack in the tension zone is close to 1 cm and eventually is destroyed by the crush of concrete at the upper edge. After the load is removed, due to the presence of the prestressed tendons, the specimen recovers part of the deformation, and the residual deformation is small.

$$l_m = 1.9c + 0.08\left(\frac{d}{\rho_{te}}\right). \quad (1)$$

For the specimen with a rust rate of 10%, the corrosion of reinforcement produced long longitudinal cracks and the distribution of cracks in the tension zone was quite irregular. Due to the influence of stirrup corrosion, the crack distribution of ordinary stirrup specimens was more complicated than that of epoxy-coated stirrup specimens and stainless steel stirrup specimens. As shown in Figure 11, in the ultimate limit state, the vertical bending moment cracks and the transverse rust-expansion cracks in the tension zone were intricately intersected, and the width of the cracks increased significantly compared with the comparison beam.

In summary, all specimens were damaged due to the crushing of concrete in the compression zone. It can be seen from the test results that the corrosion of steel bars had a great influence on the distribution of cracks during the final loading state. After the steel bars were corroded, obvious longitudinal rust expansion cracks would be produced, which made the vertical bending moment cracks and transverse rust expansion cracks intersect each other in the tension zone, and there were vertical rust expansion cracks after the stirrups were corroded.

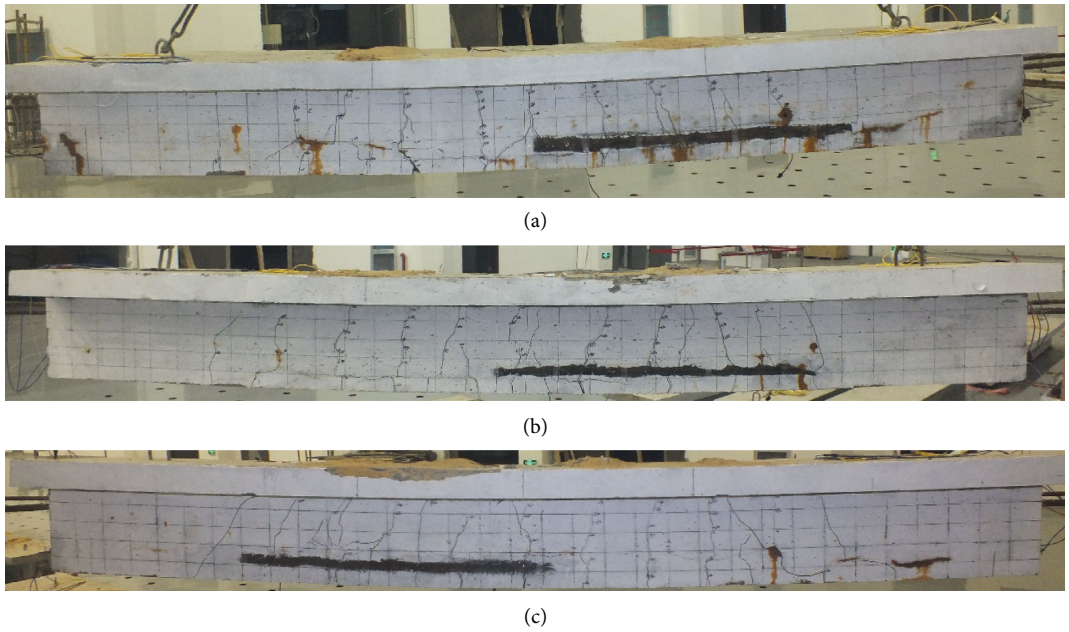

(a)

(b)

(c)

Figure 11: Cracking distribution of specimens with 10% corrosion rate. (a) 10P10, (b) 10H10, and (c) 10B10.

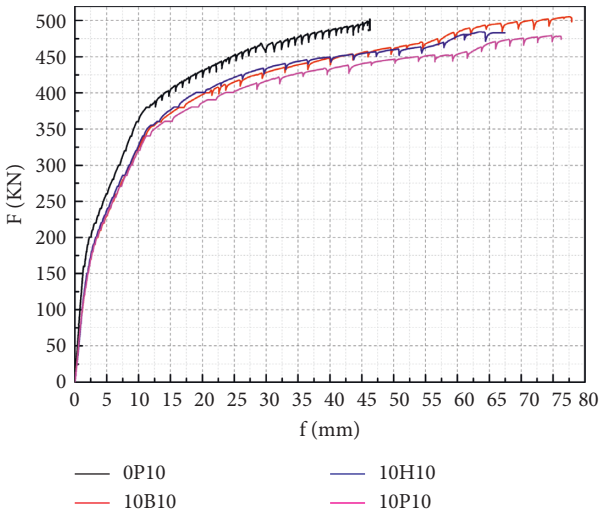

Figure 12: Load-deflection curves of the specimens.

3.2. Load-Deflection Curve and Initial Stiffness. For the contrast beam 0P10 with a thick protective layer, the position of the tension steel bar and the neutral axis was higher, so the compression zone height was lower. When the upper edge of the concrete was crushed, the deformation of the beam was very large. The load-deflection curves of the specimens are shown in Figure 12.

It can be seen from Figure 12 that the stiffness of the specimens with a corrosion rate of 10% was significantly lower than that of the contrast beam, and the deflection was significantly increased. The ultimate bearing capacity and deflection of each specimen are shown in Table 3.

It can be seen from Table 3 and Figure 12 that the corrosion of steel bars would cause a decrease in the ultimate bearing capacity, but the degree of reduction was very limited, in which the maximum reduction was only 6.1%. If factors such as manufacturing errors were taken into account, the corrosion of steel bars had almost no effect on the bearing capacity of the specimens. That was because ordinary steel bars only account for 30% of the bearing capacity

Table 3: Ultimate bearing capacity and deflection of specimens.

Number	Corrosion rate (%)	Ultimate bearing capacity (kN)	Ultimate deflection (mm)
0P10	0	508.9	53
10P10	10	478	76.2
10H10	10	484	67.5
10B10	10	504.8	77.74

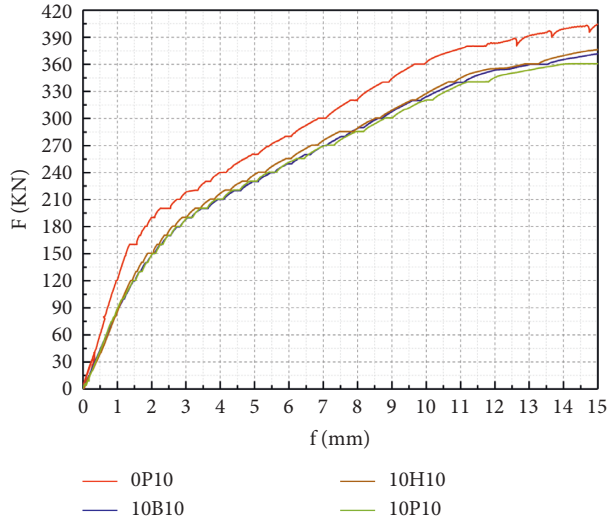

Figure 13: Stiffness at an earlier stage of specimens.

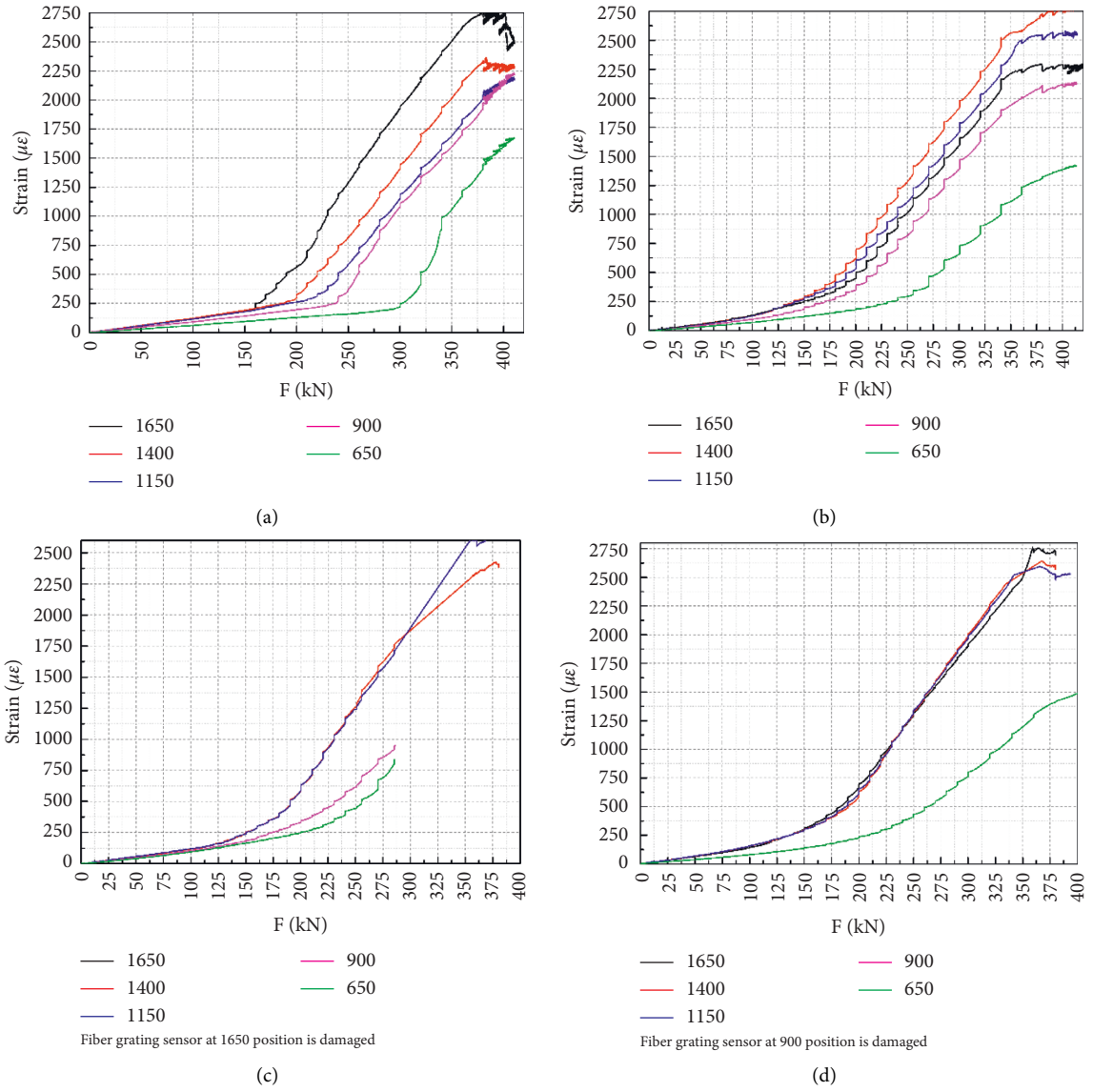

Figure 14: Load-strain curves of longitudinal reinforcement (figures in legend are the distance between measuring point and beam end, mm). (a) 0P10, (b) 10P10, (c) 10H10, and (d) 10B10.

of the specimen, and the maximum corrosion rate was only 10%. However, different types of stirrups have different effects on the ultimate load and ultimate deflection at the failure stage. The bearing capacity of stainless steel stirrups and epoxy-coated stirrups was greater than that of ordinary stirrups. This showed that stainless stirrups and epoxy-coated stirrups played a great role in preventing stirrup corrosion and the development of rust expansion cracks and inhibited the galvanic corrosion caused by the interaction between the stirrup and the longitudinal reinforcement. The ultimate bearing capacity of the stainless steel stirrup specimen was 504.8 kN, which was very close to the ultimate bearing capacity of the comparative beam (508.9 kN). Therefore, the stainless steel stirrup can effectively improve the durability of the prestressed concrete structure. In contrast, from the point of view of ultimate deflection, no matter what type of stirrup, the ultimate deflection of the specimen after corrosion had increased significantly, and it can even reach 47% for the contrast beam 0P10. This indicated that the corrosion of the steel bars would greatly reduce the overall stiffness of the prestressed structure. That was because the corrosion can cause initial rust expansion cracks in the specimens, which would ultimately affect the development and distribution of stressed cracks. However, it was worth mentioning that the limit deflection of 10H10 was small, and the effect of epoxy-coated stirrup corrosion on the overall stiffness was less than that of ordinary stirrups and stainless stirrups.

For prestressed structures, the ultimate state of bearing capacity is a very extreme state. Compared with ultimate bearing capacity, the mechanical behaviors of the structure in serviceability limit state were more worthy of attention. In fact, the impact of bond degradation and rust expansion cracking of the concrete in the tension zone was only at the

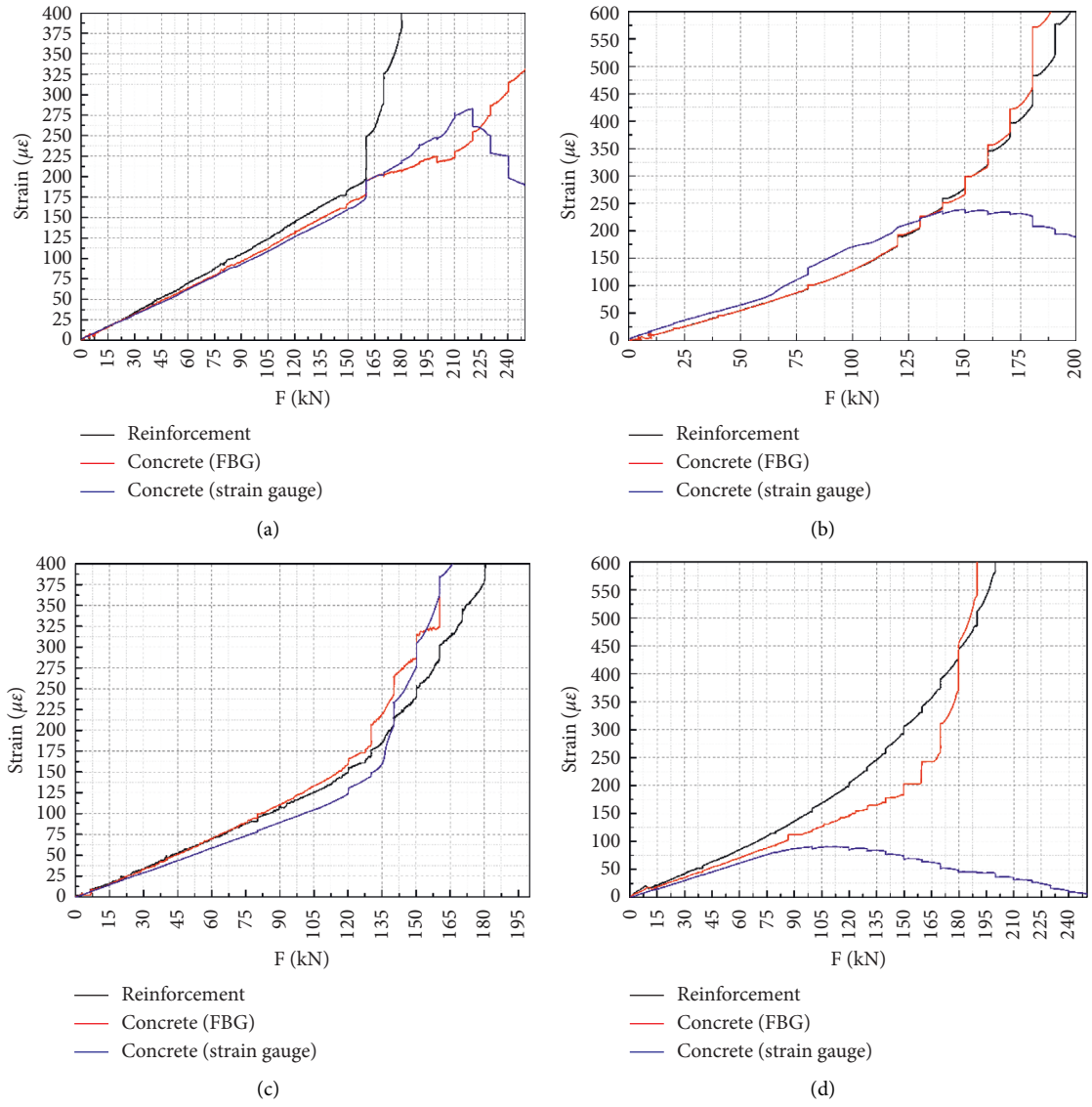

Figure 15: Strain of steel bars and concrete of specimens. (a) 0P10, (b) 10P10, (c) 10H10, and (d) 10B10.

early stage of loading. For the convenience of analysis, only the deflection curves within 15 mm before the ordinary steel bar yielded were used for comparative analysis.

It can be seen from Figure 13 that the corrosion of steel bars had a significant effect on the early stiffness and cracking load of the specimens. With the increase of corrosion rate, the early stiffness of the specimens decreased gradually. Most notably, for the specimens with a corrosion rate of 10% in this test, although the corrosion of steel bars reduced the initial rigidity, the rust expansion cracks were longitudinally long and part of the internal corrosion products had leaked out along the cracks, which did not cause further damage. This was beneficial to the initial stiffness. The test showed that the type of stirrup had very little effect on the initial stiffness, and the initial stiffness of the specimens of the three kinds of stirrups was basically the same after corrosion. Among them, the early stiffness of epoxy-coated stirrup specimens was slightly greater than that of stainless stirrups and ordinary stirrups, the load-deflection curves of stainless stirrups, and ordinary stirrups after corrosion almost overlapped, and the early stiffnesses were basically the same.

3.3. Steel-Concrete Strain. The respective strains of steel bars and concrete can be obtained by pasting optical fibers on steel bars and concrete. Before the test beam cracked, concrete and reinforcement worked together, whose deformation was coordinated. After that, the concrete tensile stress was released and the stress of the steel bar at the crack position increased.

It can be seen from Figure 14 that 0P10 had not cracked before load test, and the strain of the steel bar increased linearly with the load. For specimen 0P10, the strain of the steel bar at the midspan position was the largest, and it gradually decreased with the decline of the distance between

Table 4: Ultimate bearing capacity and deflection of specimens.

Number	Corrosion rate (%)	Cracking load (kN)	Yield load of steel bars (kN)
0P10	0	160	306
10P10	10	100	305
10H10	10	120	306
10B10	10	100	300

the longitudinal bar position and the beam end, which was consistent with the internal force distribution during the ordinary beam loading process. In contrast, the longitudinal bars of the corroded specimen 10P10 did not necessarily reach the maximum strain at the midspan section. However, due to the inhibitory effect of epoxy-coated stirrups and stainless stirrups on corrosion, the strain distribution of the longitudinal reinforcement of 10H10 and 10B10 was almost the same as that of the uncorroded specimen. From the perspective of the strain of the steel bar, for the 10% corrosion rate specimens, the corrosion had a greater influence on the section stiffness of 10B10 and 10P10 than 10H10, which was the same as the situation reflected by the load-deflection curve.

It can be seen from Figure 15(a) that in the early stage of loading (before 30 kN), the steel bars and concrete worked together; after 30 kN, the reinforcement and concrete began to have relative deformation. As the load increased, the strain difference between reinforcement and concrete became larger and larger; after 160 kN, cracks appeared in the concrete, and the stress of the steel bars around the cracks suddenly increased; with the further increase of the load, the strain of reinforcement increased nonlinearly. Although the strain of concrete increased, it was very slow. When the tensile strain of the concrete exceeded 300$\mu\varepsilon$, the concrete had already cracked. Table 4 listed all the specimen's results.

For corroded components, the strains obtained by concrete strain gauges and fiber grating sensors were quite different. Under the conditions of corrosion and ultimate load, the concrete strain gauges were damaged greatly and cannot truly reflect the changes of concrete strain. It was worth noting that during the loading process of corroded components, unlike 0P10, there was no sharp increase in steel strain. This showed that with the continuous corrosion of the steel bars, the test beams had large rust expansion cracks before loading, so the steel bars and concrete at the cracks could not deform coordinated. Even at the initial stage of loading, the corroded longitudinal bars already had greater stress.

Because the optical fiber had good capabilities of corrosion resistance and antielectromagnetic interference, the optical fiber embedded in the steel bar was not affected by the corrosion and can still reflect the relative deformation of the corroded reinforcement and concrete during the loading process. It can be seen from the test results that, compared with the comparison beam, the early straight of the whole load-strain curve of the corroded specimen was significantly shorter. Under the lower load level, the concrete had cracked, and the cracking load of 10B10 was the lowest among the three specimens. As the corrosion rate increased, the strain of corroded rebar and concrete became more complicated, and the discrepancy of data between strain gauge data and optical fiber data became larger and larger. Judging from the data obtained by the optical fiber, the strain of the steel bar of 10P10 was almost the same as the strain of concrete in the early loading stage, which had the same law as the uncorroded specimen. Among the three types of stirrup, the stainless stirrup and concrete of 10B10 underwent relative deformation under a lower load and had a larger strain difference under the same load. Therefore, although stainless stirrups can inhibit corrosion to a certain extent, they may reduce the bond force between stirrups and concrete, which increases the slip between stirrups and concrete in the early loading stage.

4. Conclusion

This article tested and analyzed the influence of different types of stirrup corrosion on the bending performance of prestressed components. A scaled model beam was designed with the 5×50 m simple-continuous box beam of the Donghai Bridge as the prototype, and the steel bars were rusted through a method of accelerating corrosion by electricity, different from other research on corrosion, and the different stirrups (three types: ordinary stirrups, epoxy-coated stirrups, and stainless stirrups) with different corrosion rate for prestressed concrete beams were studied with FBG sensor. The following conclusions were drawn through the analysis of the test results:

(1) During the loading process of corroded components, different from the corroded beam, there was no sharp increase in steel strain, that's proved with the continuous corrosion of the steel bars, and the test beams had large rust expansion cracks before cracking loading, so the steel bars and concrete at the cracks could not deform coordinated. Even at the initial stage of loading, the corroded longitudinal bars already had greater stress.

(2) The corrosion of longitudinal steel bars and stirrups can affect the final crack distribution of the prestressed structure in the ultimate limit state. Tension cracks, longitudinal rust expansion cracks, and vertical rust expansion cracks intersect each other so that the crack spacing is reduced and its width increases.

(3) For prestressed concrete structures, the corrosion of longitudinal steel bars can cause a decrease in the ultimate flexural capacity, but the degree of decrease is very limited. The flexural capacity of ordinary stirrup specimens was reduced the most, only 6.1%. Among the rusted specimens, for 10% corrosion rate of stainless stirrups, specimen has the largest flexural bearing capacity, followed by 10H10, indicating that stainless stirrups and epoxy-coated stirrups have a certain inhibitory effect on corrosion. However, corrosion will greatly increase the final deflection and reduce the early stiffness of all specimens.

(4) Corrosion of steel bars leads to failure of the bond between reinforcement and concrete. Then, the slip increases and the initial cracking load decreases. The specimen with a corrosion rate of 10% is more obvious than the uncorroded specimen in the reinforcement-concrete bond degradation, and there is no sharp increase in the stress of the reinforcement when the cracking load is brought to the beam.

(5) The strain difference between the reinforcement and concrete in the early loading stage of the corroded component is 10B10, 10H10, and 10P10 in descending order which proved the bond-slip relationship between reinforcement and concrete under the corrosion impact.

(6) It is a feasible and effective method to use FBG sensor to measure the strain of corroded steel bar and concrete because of its good working performance because optical fiber has a small impact on the surface of the reinforcements with electromagnetic interference.

Data Availability

The data used to support the findings of this study are included in the article.

Conflicts of Interest

The authors declare that they have no conflicts of interest.

Acknowledgments

This research was supported by the National Basic Research Program of China (973 Program) under Grant no. 2013CB036303.

References

[1] S. W. Tang, Y. Yao, C. Andrade, and Z. J. Li, "Recent durability studies on concrete structure," *Cement and Concrete Research*, vol. 78, pp. 143–154, 2015.

[2] P. K. Mehta, "Concrete durability-Fifty years progress," in *Proceedings of the 2nd International Conference on Concrete Durability*, vol. 49, pp. 1–32, Montreal, Canada, August 1991.

[3] F. Biondini, E. Camnasio, and A. Palermo, "Lifetime seismic performance of concrete bridges exposed to corrosion," *Structure and Infrastructure Engineering*, vol. 10, no. 7, pp. 880–900, 2014.

[4] J. M. Bian, Q. Bai, Y. M. Kang, and J. Zhang, "A review of durability research of concrete bridge," pp. 1132–113, 2013.

[5] J. Rodriguez, L. Ortega, and J. Casal, "Load carrying capacity of concrete structures with corroded reinforcement," *Construction and Building Materials*, vol. 11, no. 4, pp. 239–248, 1997.

[6] A. Shishegaran, M. R. Ghasemi, and H. Varaee, "Performance of a novel bent-up bars system not interacting with concrete," *Frontiers of Structural and Civil Engineering*, vol. 13, pp. 1–15, 2019.

[7] P. S. Mangat and M. S. Elgarf, "Flexural strength of concrete beams with corroding reinforcement," *ACI Structural Journal*, vol. 96, no. 1, pp. 149–158, 1999.

[8] S. Yang, C. Q. Fang, Z. J. Yuan, and M. Y. Yi, "Effects of reinforcement corrosion and repeated loads on performance of reinforced concrete beam," *Advances in Structural Engineering*, vol. 18, no. 8, pp. 1257–1271, 2015.

[9] D. J. Zou, T. J. Liu, and G. F. Qiao, "Experimental investigation on the dynamic properties of RC structures affected by the reinforcement corrosion," *Advances in Structural Engineering*, vol. 17, no. 6, pp. 851–860, 2014.

[10] Q. X. Shi, X. J. Li, D. T. Niu, and Y. D. Yang, "Experimental study of bearing capacity of corroded reinforced concrete eccentric compressive members," *Industrial Construction*, vol. 31, no. 05, pp. 14–17, 2001.

[11] Z. Ye, W. Zhang, and X. Gu, "Deterioration of shear behavior of corroded reinforced concrete beams," *Engineering Structures*, vol. 168, pp. 708–720, 2018.

[12] C. Higgins and W. C. Farrow, "Tests of reinforced concrete beams with corrosion-damaged stirrups," *ACI Structural Journal*, vol. 103, no. 1, pp. 133–141, 2006.

[13] G. Campione, F. Cannella, and L. Cavaleri, "Shear and flexural strength prediction of corroded R.C. beams," *Construction and Building Materials*, vol. 149, pp. 395–405, 2017.

[14] W. Zhang, Z. Ye, and X. Gu, "Effects of stirrup corrosion on shear behaviour of reinforced concrete beams," *Structure and Infrastructure Engineering*, vol. 13, no. 8, pp. 1081–1092, 2017.

[15] D. Zhang, Y. Zhao, W. Jin, T. Ueda, and H. Nakai, "Shear strengthening of corroded reinforced concrete columns using pet fiber based composties," *Engineering Structures*, vol. 153, pp. 757–765, 2017.

[16] A. K. El-Sayed, R. R. Hussain, and A. B. Shuraim, "Influence of stirrup corrosion on shear strength of reinforced concrete slender beams," *ACI Structural Journal*, vol. 113, no. 6, pp. 1223–1232, 2016.

[17] A. K. El-Sayed, "Shear capacity assessment of reinforced concrete beams with corroded stirrups," *Construction and Building Materials*, vol. 134, pp. 176–184, 2017.

[18] Z.-H. Lu, H. Li, W. Li, Y.-G. Zhao, Z. Tang, and Z. Sun, "Shear behavior degradation and failure pattern of reinforced concrete beam with chloride-induced stirrup corrosion," *Advances in Structural Engineering*, vol. 22, no. 14, pp. 2998–3010, 2019.

[19] A. Goharrokhi, J. Ahmadi, M. A. Shayanfar, M. Ghanooni-Bagha, and K. Nasserasadi, "Effect of transverse reinforcement corrosion on compressive strength reduction of stirrup-confined concrete: an experimental study," *Sadhana - Academy Proceedings in Engineering Sciences*, vol. 45, no. 1, p. 9, 2020.

[20] J. B. Mander and M. J. N. Priestley, "Observed stress-strain behavior of confined concrete," *Journal of Structural Engineering*, vol. 114, no. 8, 1988.

[21] J. B. Mander, M. J. N. Priestley, and R. Park, "Theoretical stress-strain model for confined concrete," *Journal of Structural Engineering*, vol. 114, no. 8, pp. 1804–1826, 1988.

[22] G. H. Zhang, X. H. Cao, and Q. N. Fu, "Experimental study on residual strength of concrete confined with corroded stirrups," *Canadian Journal of Civil Engineering*, vol. 43, no. 6, p. 8, 2016.

[23] L. Liu, D. T. Niu, Q. Li, and Z. He, "Stress-strain constitutive relation model of corroded stirrups confined concrete," *Jianzhu Cailiao Xuebao/Journal of Building Materials*, vol. 21, no. 5, pp. 811–816, 2018.

[24] Q. Li, D.-t. Niu, Q.-h. Xiao, X. Guan, and S.-j. Chen, "Experimental study on seismic behaviors of concrete columns confined by corroded stirrups and lateral strength prediction," *Construction and Building Materials*, vol. 162, pp. 704–713, 2018.

[25] Z. Yu, J. Li, and L. Song, "Experimental study on fatigue behaviors of PC bridge beams with corroded steel bars," *Journal of Highway and Transportation Research and Development*, vol. 31, no. 04, pp. 64–72+93, 2014.

[26] China, *Code For Design of concrete Structures 2015*, China Architecture and Building Press, Beijijng, China, 2015.